JTTEE5 8:249-257

Sealing of Thermal Spray Coatings by Impregnation

J. Knuuttila, P. Sorsa, and T. Mäntylä

(Submitted 3 June 1998; in revised form 12 January 1999)

Results from the sealing of porosity by impregnation show that below a certain wetting angle of the sealant, high penetration depths are achieved. However, only sealants with very low curing shrinkages can prevent the transport of electrolyte through the coating.

Various sealant types and impregnation methods are discussed, and factors influencing impregnation and sealing ability of sealants are reviewed. Experimental results from the sealing of plasma-sprayed aluminum-oxide coatings are presented.

Keywords coatings, corrosion, impregnation, sealing, thermal spray

1. Introduction

Moderate adhesion and a porous structure are the most often encountered problems in thermal-spray coatings that restrict their use in many applications involving corrosive media. Although most metallic consumables can be sprayed to dense coatings without open, through-coating porosity, ceramic coatings invariably contain open porosity and usually also cracks.

These structural flaws not only deteriorate the corrosion resistance of the coating-substrate system but also decrease mechanical properties and consequently the wear resistance of the coating. Although the development of higher velocity processes has decreased coating porosities, the transport of corrosive species to the substrate can still only be prevented by coating posttreatment.

Posttreatment of thermal spray coatings to close the surface porosity can be performed by laser- or electron-beam surface melting or alloying (Ref 1, 2). Also hot isostatic pressing (HIP) of the coating-substrate system can be used for densifying (Ref 3). Hot isostatic pressing not only reduces porosity but also improves mechanical properties. It is effective through the whole coating thickness but demands complex and expensive equipment. Obviously the deposition of a dense layer by another method over the porous coating can be used for sealing. High-temperature chemical vapor deposition (CVD) processes (Ref 4) and the modification, chemical vapor infiltration (CVI), using reactive gases, are other possibilities for porosity sealing. Recently metal-organic chemical vapor deposition (MOCVD) has been used for sealing oxide coatings although the results against high-temperature gaseous corrosion were not encouraging (Ref 5). More often posttreatment is performed by impregnation using polymers, inorganic solutions, or even molten metals.

In this article, factors affecting coating porosity and sealing by impregnation are reviewed. Commercial sealants, their properties, and sealing abilities were studied and compared to laboratory developed sealants using plasma-sprayed aluminum oxide as the reference coating.

J. Knuuttila, M. Sc. (Eng.), **P. Sorsa,** and **T. Mäntylä,** Tampere University of Technology, Institute of Materials Science, P.O. Box 589, FI-33101 Tampere, Finland. Contact e-mail: mantyla@cc.tut.fi. **J. Knuuttila** and **P. Sorsa** presently at Millidyne Oy, Hermiankatu 8D, FI-33720, Tampere, Finland. Contact e-mail: millidyne@hermia.fi.

2. Volume Defects in the Coating

The aim of sealing by impregnation is to close or fill all those open structural volume defects that are connected to the surface. These defects can be distinguished by their shape and means of formation as pores or cracks.

2.1 Porosity

Open or closed porosity in thermal spray coatings can originate from several different factors (Ref 6): partially or totally unmolten particles, inadequate flow or fragmentation of the molten particle at impact, shadowing effects due to lower than the optimal spray angle, and entrapped gas.

Although porosity of a coating is affected by spray equipment, spray parameters, and consumable properties, it is the application of the coating that determines the target porosity. This is especially true for ceramic coatings.

The highest wear resistance of a ceramic coating is achieved by means of a dense structure, but in large components it might be necessary to leave some porosity in the coating to relieve stresses. Also economic reasons (e.g. high throughputs) often dictate a coating process that inevitably leads to higher porosities and possibly increased microcracking through higher heat input.

Nevertheless, the application environment determines the necessity for sealing pores. If the coating itself lacks the required corrosion resistance, then sealing of the pores can still decrease corrosion by lowering the amount of reactive surface area. However, high-velocity oxygen fuel (HVOF) sprayed cermet coatings are much denser than oxide coatings, and the effect of sealing on corrosion rate of the cermet coating itself can be small. For example, WC-50NiCrSiB and WC-10Co4Cr coatings showed an enhanced corrosion rate in a saline environment, and the effect of sealing or a corrosion-resistant bond layer was small (Ref 7). Bond coats with improved corrosion resistance are often employed, but they also corrode or oxidize, although at a slower rate. Corrosion of the bond coat or the substrate leads to precipitated corrosion products (e. g., $Fe(OH)_2$) at the surface or at the coating-substrate interface, which can lead to spalling of

the coating. Because a porous coating is a natural source for crevices, it is important that the crevice and pitting corrosion resistance of the substrate and the coating be considered. Sometimes it can be more justified to choose a substrate material or bond coat with better crevice- and pitting-corrosion resistance than to try to produce coatings without open porosity (Ref 8). Electrochemical corrosion must also be taken into account with electrically conducting coatings.

2.2 Cracks and Interlamellar Bonding

Vertical and horizontal cracks originating from the spray process are typical for ceramic coatings. High cooling rates of the individual splats favor horizontal delamination between the lamellae. Poor interlamellar bonding is also typical for thermal spray coatings. It has been estimated that the bonding degree between adjacent lamellae for plasma-sprayed alumina coating is only 20 to 32%, thereby yielding horizontal cracklike defects or voids (Ref 9).

3. Impregnation Methods

Impregnation methods can be divided into four categories: atmospheric pressure impregnation, low-pressure impregnation, overpressure impregnation, and a combination of these. The choice of the impregnation method depends on the size of the coated component, required penetration depth, and the sealant, which is chosen according to the coating material and the application. Low-pressure or overpressure impregnation is suitable for small components. Only atmospheric-pressure impregnation is economically viable for larger components.

The efficiency of low-pressure impregnation is based on the removal of moisture and air from pores and cracks, thus decreasing the opposing force acting against impregnation driven by capillary pressure. This yields an increased penetration depth. Pressure level must be adjusted to the vapor pressure of the sealant to avoid excessive evaporation.

Overpressure impregnation is used mainly in cases where the sealant does not wet the coating surface; in other words, the contact angle is clearly over 90°. This is equivalent to porosity measurement by mercury intrusion porosimetry where the mercury does not wet the material and is forced into the porous structure using external pressure.

In most cases the impregnation is carried out using atmospheric pressure methods such as brushing, dipping, or spraying. The residual air inside the pores creates an opposing force, which limits sealant penetration. The effect can be decreased by formulating the sealant accordingly.

To avoid any contamination of the coating, the sealing should be performed directly after spraying when the coating is still warm but below the curing temperature. However, this is seldom practical, and the coating is usually allowed to cool down before sealing. In many cases the coating needs to be ground to achieve the final size and form tolerances. This demand forms one of the key issues in sealing. If the coating is sealed before grinding, the possibilities exist that the sealed layer might be removed by grinding or that new open porosity might be formed. On the other hand, if the coating is sealed after grinding, the grinding emulsion needs to be removed before sealing, or the sealant must match the emulsion properties in order to penetrate into the coating and displace the grinding emulsion. In some cases it is recommended that the sealing be performed both before and after grinding.

Adsorbed water not properly removed can decrease penetration depth and sealing ability of the sealant. For spraying or sealing, humidity should be controlled in all cases to keep the surface temperature above the dew point where water condenses to any surface. This might not be adequate since water from humid air can be adsorbed into the coating through a capillary condensation phenomenon, and such water is extremely difficult to remove from small pores.

4. Sealants

Sealants for impregnation can be designated organic sealants, inorganic sealants, and metals. Their general properties are considered in the following, and organic sealants are reviewed in more detail.

In sealing the aim is to seal the porosity to as great a depth as possible. However, there are applications where only a relatively thin sealed layer is considered optimum. In thermal barrier coatings (TBCs), a relatively high amount of porosity and cracking are needed for thermal insulation and thermal shock resistance. At the same time, however, these characteristics make the coating permeable for corrosive gases and liquids. Thus, the goal is to seal only the surface layer. Another example for a low penetration depth is arc or wire flame spraying of aluminum for offshore corrosion protection where the sealer should not penetrate deeper than about 25 μm to maintain the cathodic protection ability of the coating (Ref 10).

4.1 Organic Sealants

Typically organic sealants are one- or two-component unfilled resin systems formulated for suitable viscosity and surface tension. Formulation is usually done by using solvents, reactive diluents, or surfactants. In one component, systems curing is catalyzed by heat, ultraviolet light, or high-energy radiation such as electron beam (EB) or laser radiation. In two-component systems the cross linking is activated by curing catalysts. The often-used organic sealants are based on epoxies, phenolics, furans, polymethacrylates, silicones, polyesters, polyurethanes, and polyvinylesters. Waxes can be used also. For thermal spray aluminum coatings, aluminum-filled vinyl and silicone sealers for extended cathodic protection are also used (Ref 10).

Few detailed publications exist about sealing of thermal spray coatings by organic sealants (Ref 11, 12). In many publications, the information about sealants or experimental procedure is inadequate. For example, it might not be stipulated whether the inevitable surface film left by the sealant should be removed before making corrosion measurements. Essential information such as how the samples were treated before impregnation and how long the impregnation time was are often unmentioned as well.

In an interesting review by E. Lugscheider et al. (Ref 11), bond strengths of unknown coatings were decreased by sealing. This was believed to be due to entrapped air and evaporated byproducts or solvents from the sealant, which were in compres-

sion at the substrate-coating interface due to raised capillary pressure. The effectiveness of several sealants for protecting plasma-sprayed Al_2O_3-13TiO_2 and flame-sprayed chromium-steel coatings against corrosion by sulfur dioxide salt spray and oscillation wear were investigated in another study (Ref 12). Electric insulation resistance was also used as a measure of sealant effectiveness in alumina-titania coatings. Metallographical investigation was used to evaluate the penetration depth, which was found to vary between 23 and 40 μm depending on the sealant. Polyurethane- and epoxy-based sealants yielded the highest corrosion resistances. After grinding a 100 μm layer from the sealed samples, corrosion and insulation resistances reduced in all cases. Wear resistance was also improved by sealing (Ref 12). Epoxy impregnation of water-stabilized plasma-sprayed aluminum oxide freestanding deposits greatly improved the Young's modulus and made the coatings impermeable for gases, although the effect on total porosity was small. It was deduced that the resin had sealed only the necks between larger pores and interlamellar cracks or voids, thus improving cohesion (Ref 13).

4.2 Inorganic Sealants

Inorganic sealants are usually aimed for high-temperature applications. Typically, they also reacted to solid material at elevated temperatures. Besides aluminum phosphates and sodium and ethyl silicates, various sol-gel type solutions and chromic acid have been used for sealing purposes. Inorganic sealants are normally used for preventing corrosion by molten salts, metals, and even aggressive gaseous species, but earlier results of this study also have shown that a high level of strengthening and improvement in wear resistance can be achieved using aluminum-phosphate-based sealants (Ref 14, 15). In many burning processes the coatings are exposed to corrosive gases that easily penetrate through the coating. Besides physical blocking of this path by a corrosion-resistant sealant, one possibility for sealing the coatings could be the impregnation of pores with a material that would react with the corroding species to create an active barrier against deeper penetration.

Aluminum Phosphate. Acid aluminum phosphates have long been known as refractory binders. With suitable formulation they can also be used as refractory sealants, especially for ceramic coatings. This study showed tremendous improvements in dry abrasion resistance of thermal spray oxide coatings when using aluminum-phosphate-based sealants (Ref 14, 15). The effect is based on the fact that the phosphate acts as a refractory glue that forms solid bridges over pores and cracks. Aluminum phosphate sealing also has a beneficial effect in transferring the residual stress state of the coating toward compression, thus enhancing wear resistance. However, the effect can vary for different coatings and wear modes (Ref 16). The method is particularly attractive in upgrading low quality oxide coatings produced, for example, by flame spraying or strengthening and sealing of freestanding porous-oxide components. The optimum heat treatment temperature to $AlPO_4$ can vary from 180 to 400 °C, depending on the phosphate formulation and coating material, which also participates in the reaction.

Recently water-stabilized plasma-sprayed freestanding aluminum oxide coatings were sealed with aluminum-phosphate-based solution. The sealant penetrated through the 3 mm thickness although its concentration in the middle was only 40% of that at the surface as determined by scanning electron microscopy/energy dispersive spectroscopy (SEM/EDS). A large improvement in Young's modulus was detected after annealing (Ref 13).

Sol-Gel. Sol-gel coatings or treatments refer to the formation of a stable sol, the hydrolyzing of the sol to a gel, and the calcining of the gel at elevated temperature to oxide. The sol can include a variety of metal alkoxides, nitrates, or hydroxides, which can be transformed to gel-like structure. This results in very reactive nanoscale oxide particles.

To seal the top layer of a yttria-stabilized ZrO_2 TBC, prehydrolyzed ethyl silicate containing 25 wt% SiO_2 was used. After heat treatment at 1200 °C in a furnace or by an arc lamp, a silica-infiltrated layer with reduced porosity and high hardness was formed. For this particular system the penetration depth, d, was found to depend on infiltration time, t, as follows: $d = 0.04\ t^{0.25}$ (Ref 17).

Also aluminum isopropoxide in isopropyl alcohol was used as the sol for sealing ZrO_2-8Y_2O_3 coatings, after which hydrolyzation to a gel by immersing the specimens in water was performed. The alumina gel decomposed to γ-aluminum oxide after drying and heat treatment at 600 °C. Gas permeability and current density through the coating in NaCl electrolyte decreased as the infiltration time was increased (Ref 18).

In another study, aqueous aluminum hydroxide sol, zirconium butoxide in butanol, and zirconium and yttrium acetates in dilute acetic acid were used for impregnating freestanding ZrO_2-8Y_2O_3 coatings under a low pressure. Specimens were calcined at 600 °C and heat treated at 1000 °C to achieve corresponding oxides. The whole coating thickness could be infiltrated using the aluminum hydroxide sol.

However, the largest pores were not completely filled, which can be understood by the equation for capillary pressure shown in section 5, "Impregnation Theory." The sol did not form solid material filling the pores. Instead it formed nanosized α-alumina grains or particles on the pore surfaces (Ref 19). Ultrasonic treatment was used to aid the infiltration of hydrolyzed aluminum tri-isopropoxide gel into alumina coatings. Calcining was performed at 400 °C after which open porosity (as studied by electrochemical methods) was reduced (Ref 20).

4.3 Molten Metals

Molten metals also have been used for sealing and strengthening purposes. Copper infiltration has been performed by melting a copper foil on a plasma-sprayed Ti-30Mo coating, which increased coating adhesion, wear resistance, and corrosion resistance against HCl and H_2SO_4 solutions (Ref 21). In the same manner, molten manganese has been infiltrated in a vacuum furnace into plasma-sprayed alumina and zirconia-8 wt% yttria coatings. High-penetration depths were achieved, and in the case of an alumina coating, $MnAl_2O_4$ reaction products were formed. A large increase in coating hardness (and in the case of zirconia, also in fracture toughness) was obtained for both coatings (Ref 22). In a further study various manganese-copper alloys were employed for vacuum furnace melting and sealing of zirconia-8 wt% yttria coatings. Contact angles and capillary pressures for various molten manganese-copper alloys were also measured and calculated. The results showed that zirconia

was completely wetted by pure manganese. Alloying with copper decreased the wetting until at 80% of copper the wetting angle was 113°, and the liquid did not penetrate into the coating. This infiltration improved mechanical properties distinctly as shown also in a previous investigation (Ref 3). Infiltration by copper electroplating has been used to reveal microcrack patterns and to study interlamellar bonding in a plasma-sprayed alumina coating. However, any effect on coating properties was not reported (Ref 9).

4.4 Sealant Properties

The sealant when in a liquid state must possess several properties to be effective; that is:

- It has to penetrate deep enough into the coating.
- The curing system must be related to the component size (i.e., large components cannot be oven-cured).
- The sealant must be stable against phase separation by capillary forces during penetration.
- The curing shrinkage must be the smallest possible.
- Environmental factors must be considered because solvent evaporation is not desirable.
- Possible solvents must be removed properly from the curing sealant to avoid softening.
- The sealant needs to form only a thin surface film to avoid extra postgrinding.

In the solid state the sealant must accomplish the following:

- Exhibit chemical durability against the environment
- Have low diffusion of electrolyte and oxygen through the sealant
- Have good adhesion to the coating
- Have the necessary temperature resistance
- Retain or improve functional properties of the coating surface
- Create minimum amount of tensile stress in the coating

The last note can be explained as follows. If the strength of the sealant develops after adhesion to the pore wall has occurred and the sealant has high curing shrinkage, then it can create local tensile stresses and cause cracks in low-modulus, brittle coatings. This phenomenon can occur especially with organic sealants, which must be cured at elevated temperatures where the cross linking starts from the pore walls. Enhancing the effect is the fact that polymers have a high coefficient of thermal expansion (CTE) compared to ceramic or metallic coatings and tend to shrink more when cooling from curing temperature. If adhesion to the coating is higher than the cohesion of the sealant, then cracking can occur in the sealant if the curing shrinkage exceeds a certain limit.

Besides physical hindrance created by the sealant, the electrolyte transport in wet corrosion is affected by the chemical resistance of the sealant and the diffusion of electrolyte through the sealant. In the case of organic sealants, low cross-link density, low crystallinity, high polarity of the polymer, and high ambient temperature in relation to the glass transition temperature, T_g, all favor the diffusion of water molecules through the polymer. Diffusion rates can be greatly reduced when polarity is achieved through nonhydrophilic groups.

In addition, environmental factors, health factors, and the user friendliness of the sealant system need to be considered. Two-component systems with their limited shelf life can suit for batch processing but not for continuous use. Sealants that are based on evaporation of the solvent cannot be used without proper treatment of the fumes. Catalyzed sealants can cause inconsistencies in penetration depth due to the gradual change in viscosity. Although such development is directed toward water-based sealants, much work remains in achieving sealing properties comparable to fully organic sealants. Ultraviolet-curable sealants are also very practical due to the ease of curing at room temperature.

5. Impregnation Theory

Interfacial surface tension and application viscosity are important properties of a sealant that largely determine the penetration depth and velocity. A third important property is the curing shrinkage, which determines the ability of a sealant to physically prevent transport of corroding substances to the substrate.

The driving force for a sealant to penetrate into the coating is capillary force, which can be described as the pressure difference, ΔP, using the Young-Laplace equation in the case where the liquid does not completely wet the capillary:

$$\Delta P = \frac{2\gamma_{LV}\cos\theta}{r} \qquad \text{(Eq 1)}$$

where γ_{LV} is surface tension of the sealant, θ is the wetting angle, and r is the capillary radius. To clarify the importance of interfacial surface tension Eq 1 can be written:

$$\Delta P = \frac{2(\gamma_{SV} - \gamma_{SL})}{r} \qquad \text{(Eq 2)}$$

where γ_{SV} is the surface tension between the solid and the vapor and γ_{SL} the surface tension between the solid and the liquid.

Since it is not usually possible to choose the surface energy of the solid, the goal is to decrease the interfacial surface tension between the solid and the liquid, γ_{SL}, for improved penetration of the sealant.

However, the rate of penetration depends also on the viscosity η of the sealant and, according to Washburn, for a liquid displacing air from capillary:

$$v = \frac{r\gamma_{LV}\cos\theta}{4\eta L} \qquad \text{(Eq 3)}$$

where v is the penetration velocity and L is the distance from the surface. The first equation indicates that the smaller the pore diameter is, the deeper the sealant penetrates if other parameters are kept constant. This indicates that the penetration depth and pore-filling ability of a particular sealant depends on the pore size distribution of the coating.

These simplified models do not take into account that the capillaries or pores in coatings are in fact closed from the other end. The residual air in the pore or evaporating gases from the

sealant create an opposing force to capillary pressure and limit the flow of sealant. In the case of air or water in the pores, it is important that the interfacial surface tension between the sealant and air, γ_{LV}, or between the sealant and water, γ_{LL}, is small for increased penetration. Because evaporation starts before curing, the raising pressure can push viscous sealant backwards and cause a decreased sealing effect. In addition, the contact angle of a moving meniscus differs from the contact angle of a static one, especially at higher temperatures, and this can cause experimental misinterpretations. Surface roughness is also a factor influencing the measured wetting angles and is a possible measurement error. It can be concluded that impregnation is a complex dynamic phenomenon governed by several surface and bulk properties of the sealant and the coating.

6. Experimental

The goal of sealing by impregnation is usually to improve corrosion resistance of the porous coating-substrate system. However, it is important to know how the sealant affects the mechanical properties of the coating (especially the wear resistance) for various applications. The experimental section summarizes some recent results concerning the sealing of plasma-sprayed alumina coatings. The sealing efficiency of different sealants was studied by electrochemical measurements and wear testing.

6.1 Coatings

The alumina coatings from Amperit 740.1 powder (H.C. Starck GmbH, Germany) were produced by atmospherically plasma spraying using Plasmatechnik A3000S F4 plasma-spray system equipped with 6 mm anode (Plasmatechnik GmbH, Switzerland). Spray parameters are presented in Table 1.

Spray distance was 110 mm, surface speed was 75 m/min, distance between passes was 5 mm, and the powder port diameter was 1.8 mm. Air cooling was used to keep the coating temperature below 180 °C during spraying. The thickness of one pass was 9 μm.

The substrate material for the rubber wheel abrasion tests was Fe 52, and in electrochemical polarization measurements 25CrMo4 was used. The size of the specimens for these tests were 20 by 20 by 50 mm and 6 by 22.5 mm diameter, respectively. To ensure constant conditions, all the substrates for different tests were sprayed at the same time using a rotating specimen holder.

6.2 Studied Sealants

Several commercial and laboratory developed sealants were employed. Their properties and curing procedures are listed in Table 2. Wetting angles for ground alumina coatings were measured using optical charge-coupled device camera-based wetting-angle measurement equipment. The dry grinding for wetting angle measurements was made using 800 grit SiC paper. The image was digitized and wetting angles were calculated using PISARA software (Fotocomp Oy, Finland). Dynamic viscosities of the sealants were measured using the Höppler viscosimeter according to SFS 3758 (Ref 24) at room temperature. Curing shrinkage was measured from the mass and volume changes of the hardened samples cast into polytetrafluoroethylene (PTFE) molds. Note that the solvent-based sealant D does not shrink because it forms a polymeric material by coalescence and not by cross linking.

Sealing was performed after coatings had cooled to room temperature. Light brushing with a nylon brush was the only precleaning procedure for the coatings. Sealants were prepared just before application and applied by brushing. All sealants were applied only once, except sealant D, which was applied three times and cured as described in Table 2. The sealants were allowed to impregnate for 15 to 30 min before curing. The com-

Table 1 Spray parameters for plasma-sprayed alumina coatings

Powder	Particle size, μm	Current, A	Voltage, V	Plasma forming gases, slpm		Argon carrier gas, slpm	Feed rate, g/min
				Ar	H_2		
Amperit 740.1	–45 + 22.5	610	71	41	14	3.9	25

slpm, standard liters per minute

Table 2 Sealants and their properties

Sealant	Base polymer	Curing parameters	Wetting angle on γ-alumina, degrees	Viscosity, η, mPa/s	Curing shrinkage by weight %	Curing shrinkage by volume %
A	Inorganic aluminum phosphate	200 °C/7 h	97	505	48	…
B	Methacrylate(a)	60 °C/1 h	15	6.5	3.8	17.6
C	Methacrylate(a)	60 °C/1 h	15	8.6	2.6	5.3
D	Phenol(a)	RT	10	1.5	79.6	8
E	Epoxy	80 °C/2 h	39	162	0.1	0.2
F	Methacrylate(a)	UV	26	28	0.5	<2
G	Epoxy	60 °C/2 h	42	179	1	0.1
H	Furan	60 °C/1 h – RT	67	626	2	2
I	Vinyl ester	60 °C/1 h – RT	83	319	0.6	2.4

(a) Commercial sealant

mercial sealants aimed for sealing of thermal spray coatings are marked with (a) in Table 2.

Commercial sealants B, C, and D exhibited very low viscosities and wetting angles but high volume curing shrinkages compared to laboratory-formulated sealants E to I. Low wetting angle and viscosity promote penetration of the sealant into the coating.

6.3 Coating Microstructure

The coatings were characterized by x-ray diffraction, optical microscopy, and by SEM/EDS. Coating microhardness was determined and porosity was calculated by image analysis from carefully polished cross sections of the coatings. Open porosity was determined by the water immersion method according to EN 623-2 (Ref 25) for freestanding coatings. Image analysis yielded a relatively high level of porosity compared to the water immersion method, which indicates the presence of pullouts due to metallographic preparation (Table 3). Image analysis also measures the closed porosity, but the smallest pores cannot be detected due to limitations of optical microscopy.

Alumina coating consisted mainly of γ-Al_2O_3; only minor peaks of unmolten α-Al_2O_3 particles were detected. The aluminum phosphate sealing produces a layer of different crystalline orthophosphates, metaphosphates, and hydrated orthophosphates on the coating surface. A minor amount of $AlPO_4$ was still detected after grinding a 100 μm layer from the as-sprayed alumina surface.

Table 3 Porosity and hardness of the as-sprayed coating

Coating	Porosity(a), %	Open porosity(b), %	HV0.3
Al_2O_3	7.7 ± 0.5	5.2 ± 0.1	915 ± 56

(a) As measured by image analysis. (b) As measured by water immersion

6.4 Dry Abrasion

The abrasion resistance of the sealed alumina coatings was evaluated using a modified ASTM G 65-94 (Ref 26) rubber wheel abrasion equipment. Angular quartz sand with particle size of 0.1 to 0.6 mm was used as the abrasive, which was fed between the rotating rubber wheel and the specimen. The test length was 5904 m and the specimen load was 13 N.

As is seen from the results in Fig. 1, the dry abrasion behavior depended very much on the sealant. The organic sealants E, F,

Table 4 Thickness and maximum current density of as-sealed and ground alumina coatings

Sealant	As-sealed, μm	After grinding, μm	Removed thickness in grinding, μm	Maximum current density for sealed samples, μA/cm²	Maximum current density for sealed and ground samples, μA/cm²
Reference	358	…	…	10,000	…
A	330	180	178	8.3-11	4200-4700
B	354	194	164	3000-3400	4100-4700
C	356	186	172	2.8	0.0028
D	358	191	167	0	11.6-14.8
E	363	174	184	0.011	0.0011
F	346	194	164	0	0.0011
G	352	210	148	0	0
H	338	215	143	13.4-16.0	0.23
I	358	220	138	406-462	1376-1667

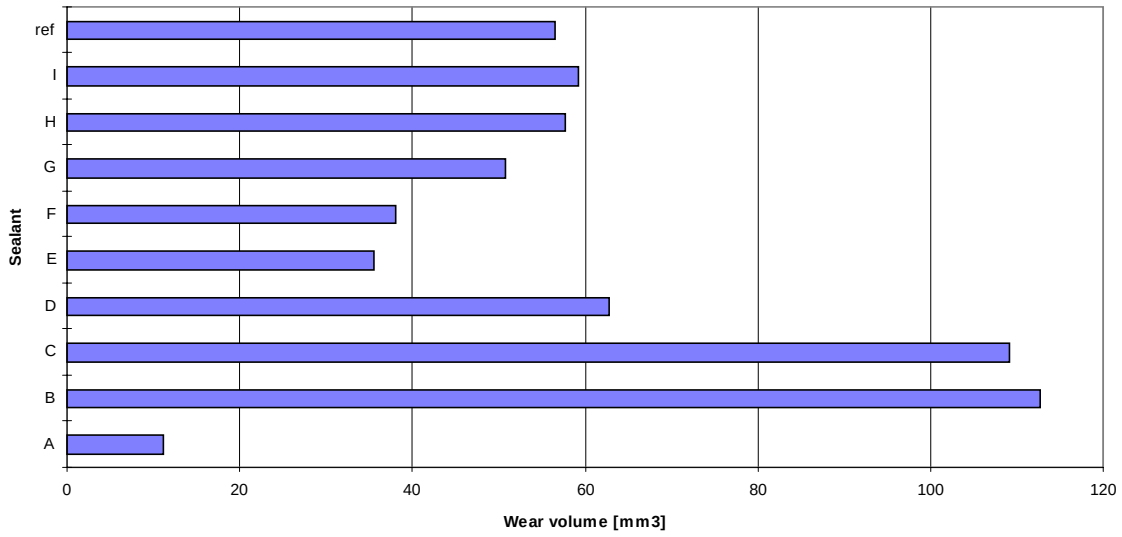

Fig. 1 Dry abrasion wear of the sealed coatings measured as volume loss. Ref indicates as-sprayed coating without sealant.

and G decreased wear, while H and I revealed a minor effect. Surprisingly, samples sealed with sealants B, C, and D showed higher wear than the unsealed samples. As shown in previous studies, aluminum phosphate sealing, A, is a very effective strengthening method, which also improves the dry abrasion resistance (Ref 14, 15).

The reason for this differing behavior with various sealants might lie in the fact that the sealants penetrate, shrink, and adhere to pore walls differently. If the sealant penetrates and adheres well into the coating but has a high shrinkage in curing, it can create local tensile stress fields causing easier and larger wear-particle detachment. Looking at the curing shrinkages in Table 2 shows that indeed those sealants B, C, and D, which displayed the highest wear, also exhibited the highest curing shrinkages. Although the sealant D has higher shrinkage than sealant C, it was hardened at room temperature and exhibited poorer mechanical properties than sealants B and C. In tension the sealant yields, thereby exhibiting its lower effect on decreased wear resistance.

Obviously, the more pores are filled with the sealant, then the more weight loss is recorded with the same volume loss although the effect is small with these porosity levels and sealant densities. If the sealant has a strengthening effect on the coating, its effectiveness depends on coating porosity. Recent studies have shown that an important factor in increased wear resistance in aluminum phosphate-sealed oxide coatings is the change in residual stress state toward compression.

6.5 Electrochemical Measurements

Because the penetration depth of a sealant is always limited, it is important to know how thick a surface layer can be removed or worn without sacrificing corrosion resistance. As pointed out earlier, rough grinding can also open new pores and create cracks extending through the coating.

The barrier properties of the sealants were studied for both sealed specimens and for sealed and ground specimens by electrochemical polarization measurements. Barrier properties were compared to those for unsealed and unground alumina coatings. The measurements were performed using EG&G Potentiostat/Galvanostat Model 273A (EG&G Instruments, Princeton, NJ). Neutral solution containing 3.5% NaCl in deionized water was used as the electrolyte. The electrode potential was raised from –1000 mV to 1000 mV with the rate of 0.5 mV/s, and the current density that flowed through the coating-substrate system was recorded. An Ag/AgCl electrode was used as the reference electrode and platinum as the counter electrode. A stabilization period of 300 s was used before starting the measurement. Because alumina is an insulator, any current flowing in the system is due to electrolyte penetration through the coating to the substrate. The electrolyte was in contact only with the coated surface. The round contact area was in all cases 1.17 cm^2.

A thin residual sealant film exists at the surface after sealing. The film was removed from half of the coatings by light grinding with dry 120 grit SiC paper before measurements to reveal the true coating surface with free alumina surface. The other half of the sealed coatings was ground with a diamond wheel so that 140 to 180 μm of the coating was removed. The grinding parameters were 2 m/min table speed and 10 μm cut depth. The grinding lubricant was Grade Shell KA Fluid Blue (Shell, Holland) 1 to 20 in water. The diamond wheel type was D126R75BX400 (Ventiboart, Belgium). After SiC paper grinding and diamond grinding, the surface was wiped clean with acetone and dried by blowing air.

In Table 4 the thickness of the coatings as measured by optical microscopy together with the maximum current densities are presented. High current densities indicate a large volume of open porosity and, thus, high corrosion rates. The detection limit of the equipment for current density was 0.0006 μA/cm^2. This is indicated as 0 in Table 4.

The results show that after sealing, sealants D, F, and G produced totally dense coatings. After grinding, only the coating sealed with sealant G was completely dense, although the cur-

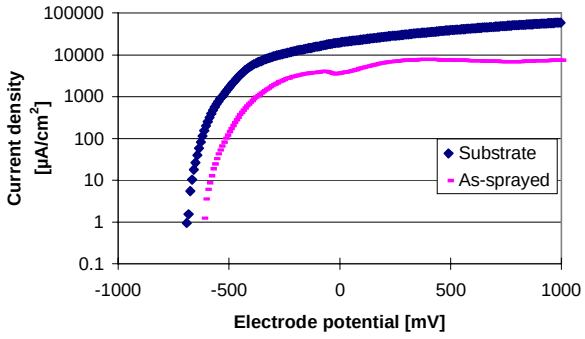

Fig. 2 Current density of the substrate material and as-sprayed coating as a function of electrode potential

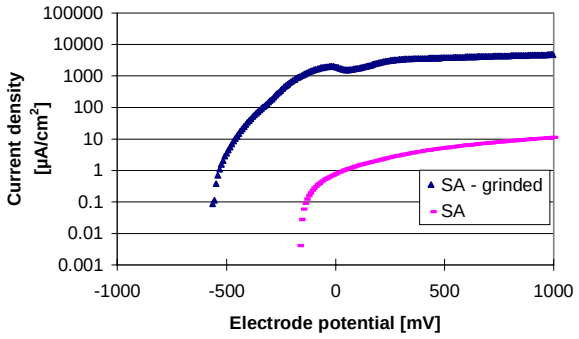

Fig. 3 Current density of the aluminum phosphate sealed and ground alumina coating

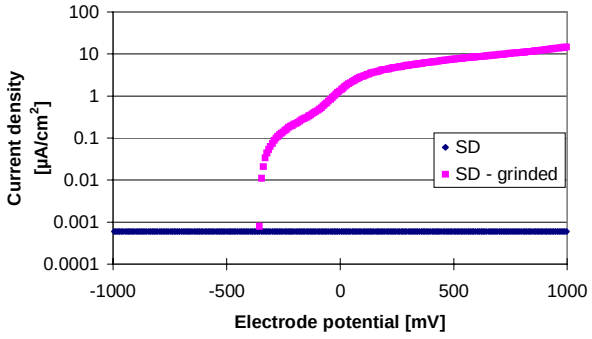

Fig. 4 Current density of the alumina coating sealed with sealant D after and before grinding

rent densities with sealants E and F were also very small. This probably arises from the fact that these sealants exhibited the smallest curing shrinkage although their wetting angles on alumina and viscosity were higher than those for commercial sealants B, C, and D.

It is interesting to note that the current densities after grinding were smaller than densities in unground specimens for sealant C, E, and H. This could be due to the fact that the residues from grinding might have closed pores at the surface or that the sealant has swelled due to water intake from the grinding emulsion.

In Fig. 2 to 4 typical electrode potential-current density curves are shown. As shown in Fig. 2, the alumina coating itself does not protect the substrate from corrosion although the maximum current density was one tenth of that for the plain substrate.

Aluminum phosphate sealing is already more effective in lowering the corrosion rate to almost 1/1000 from unsealed coating (Fig. 3). However, after grinding of a 178 μm layer from the sealed surface, the current density or corrosion rate had reached the original value of an unsealed sample, thereby indicating that much of the aluminum phosphate was removed by grinding. Our earlier results indicate that aluminum phosphate penetrates deeper if it is allowed to impregnate before hardening; but this may be difficult due to the higher viscosity of aluminum phosphate. It should be noted that the corrosion potential has transferred from over –500 mV to –200 mV indicating a change in corrosion reaction at the substrate-coating interface.

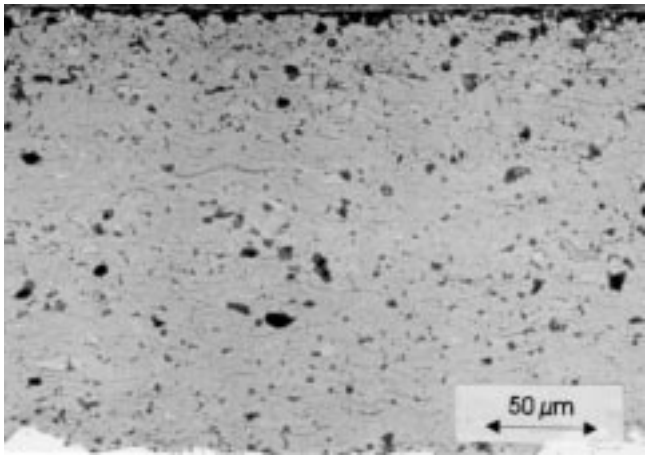

Fig. 5 Optical micrograph of alumina coating sealed with sealant G after grinding. Filled pores are slightly visible. 270×

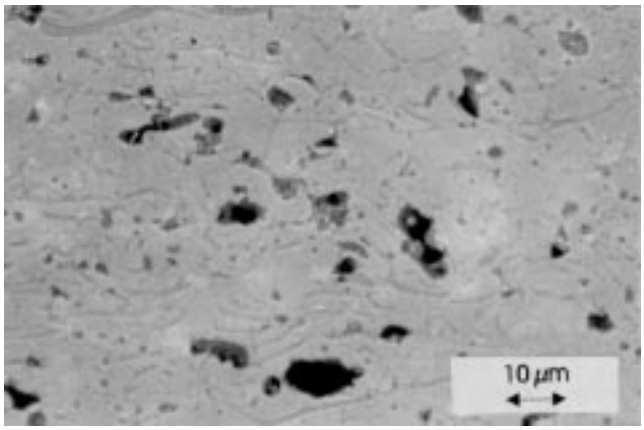

Fig. 6 Larger magnification from Fig. 5 showing smaller completely filled pores and larger partially filled pores. 680×

In Fig. 4 the effect of grinding on the permeability of the coating sealed with sealant D is seen. Grinding with a diamond wheel had either removed most of the sealant or opened new pores extending to the substrate, as can be seen from the maximum current densities reaching a value of 14.8 $\mu A/cm^2$.

After diamond wheel grinding, only sealant G showed impermeability against electrolyte diffusion, being constantly flat throughout the voltage range. This indicates that grinding does not open any new pores extending to the substrate, which could destroy the corrosion resistance of the sealed coating.

Fully sealed small pores through almost the whole coating along with only partially filled large pores can be observed from the optical micrographs of coating with sealant G (Fig. 5, 6). The coating thickness after grinding is 210 μm and indicates that the penetration of the sealant has been 250 to 300 μm. The reason for only partial filling of larger pores is due to reduced capillary pressure in larger capillaries or pores as already shown in Eq 1.

7. Conclusions

According to the theory of capillary pressure, it appears that a low interfacial surface tension between the coating and the sealant is the most important factor dictating the penetration depth. The pore size distribution of the coating is equally important; larger pores might not become filled due to lowered capillary pressure. Static wetting angle measurements alone might not provide enough information on dynamic wetting angles, which depend on velocity.

However, according to results of this study on plasma-sprayed alumina coatings, it seems that below a certain static wetting angle (approximately 45°), the sealant penetrates sufficiently deep into the coating. To ensure impermeability it is more important that curing shrinkage is the smallest possible. Allowing the sealant to impregnate long enough to ensure adequate penetration is important in using high-viscosity sealants. In the case of plasma spraying it is also important to note that grinding of the alumina coating does not necessarily open new pores or cracks extending to the substrate.

Alumina was used here as the model coating, but in each case the choice of the sealing method, sealant, and the sealing time must be separately evaluated, depending on the coating material, pore size distribution, component size, finishing procedure, and the application.

Acknowledgment

The assistance of Ms. R. Tolvanen in experimental work is gratefully acknowledged.

References

1. K.M. Jasim, R.D. Rawlings, and D.R.F. West, Characterization of Plasma-Sprayed Layers of Fully Yttria-Stabilized Zirconia by Laser Sealing, *Surf. Coat. Technol.*, Vol 53, 1992, p 75-86
2. A. Petitbon, L. Boquet, and D. Delsart, Laser Surface Sealing and Strengthening of Zirconia Coatings, *Surf. Coat. Technol.*, Vol 49, 1991, p 57-61

3. K.A. Khor, Hot Isostatic Pressing Modifications of Pore Size Distribution in Plasma Sprayed Coatings, *Mater. Manuf. Process.*, Vol 12 (No. 2), 1997, p 291-307
4. T. Mäntylä, P. Vuoristo, and P. Kettunen, Chemical Vapor Deposition Densification of Plasma Sprayed Oxide Coatings, *Thin Solid Films*, Vol 118, 1984, p 437-444
5. V.A.C. Haanappel, J.B.A.Scharenborg, H.D. van Corbach, T. Fransen, and P.J. Gellings, Can Thermal Barrier Coatings be Sealed by Metal-Organic Chemical Vapor Deposition of Silica and Alumina?, *High Temp. Mater. Process.*, Vol 14 (No. 2), April 1995, p 57-66
6. *Plasma-Spray Coating, Principles and Applications*, R.B. Heimann, Ed., VCH Verlagsgesellschaft, Weinheim, 1996, p 164-165
7. A. Neville and T. Hodgkiess, Corrosion Behavior and Microstructure of Two Thermal Spray Coatings, *Surf. Eng.*, Vol 12 (No. 4), 1996, p 303-312
8. A.A. Ashary and R.C. Tucker, Jr., Electrochemical and Long-Term Corrosion Studies of Several Alloys in Bare Condition and Plasma Sprayed with Cr_2O_3, *Surf. Coat. Technol.*, Vol 43/44, 1990, p 567-576
9. A. Ohmori and C.-J. Li, Quantitative Characterization of the Structure of Plasma-Sprayed Al_2O_3 Coating by Using Copper Electroplating, *Thin Solid Films*, Vol 201, 1991, p 241-252
10. S.L. Wolfson, Corrosion Control of Subsea Piping Systems Using Thermal Sprayed Aluminum Coatings, *Mater. Perform.*, July 1996, p 32-38
11. E. Lugscheider, P. Jokiel, V. Messerschmidt, and G. Beckschulte, Subsequent Sealing of Thermal Spray Coatings to Increase Corrosion Resistance, *Surf. Eng.*, Vol 10 (No. 1), 1994, p 46-51
12. B. Wielage, U. Hofmann, S. Steinhäuser, and G. Zimmermann, Improving Wear and Corrosion Resistance of Thermal Sprayed Coatings, *Surf. Eng.*, Vol 14 (No. 2), 1998, p 136-138
13. P. Chraska, V. Brozek, B.J. Kolman, J. Ilavsky, K. Neufuss, J. Dubsky, and K. Volenik, Porosity Control of Thermal Spray Ceramic Deposits, *Thermal Spray—Meeting the Challenges of the 21st Century*, C. Coddet, Ed., ASM International, 1998, p 1299-1304
14. K. Niemi, P. Sorsa, P. Vuoristo, and T. Mäntylä, Thermal Spray Alumina Coatings with Strongly Improved Wear and Corrosion Resistance, *Thermal Spray Industrial Applications*, C.C. Berndt and S. Sampath, Ed., ASM International, 1994, p 533-536
15. E. Leivo, M. Vippola, P. Sorsa, P. Vuoristo, and T. Mäntylä, Wear and Corrosion Properties of Plasma Sprayed Al_2O_3 and Cr_2O_3 Coatings Sealed by Aluminum Phosphates, *J. Therm. Spray Technol.*, Vol 6 (No. 2), 1997, p 205-210
16. J. Knuuttila, S. Ahmaniemi, and T. Mäntylä, Wet Abrasion and Slurry Erosion Resistance of Thermal Spray Oxide Coatings, *Nordtrib '98: Proc. 8th International. Conf. Tribology*, S. Eskildsen, D. Larsen, H. Reitz, E. Bienk, and C. Straede, Ed., Danish Technological Centre, Aarhus, Denmark, 1998, p 873-880
17. I. Berezin and T. Troczynski, Surface Modification of Zirconia Thermal Barrier Coatings, *J. Mater. Sci. Lett.*, Vol 15, 1996, p 214-218
18. G. John and T. Troczynski, Surface Modification of Thermal Sprayed Coatings, *Thermal Spray: Practical Solutions for Engineering Problems*, C.C. Berndt, Ed., ASM International, 1996, p 483-488
19. J. Kathikeyan, C.C. Berndt, A. Ristorucci, and H. Herman, Ceramic Impregnation of Plasma Sprayed Thermal Barrier Coatings, *Thermal Spray: Practical Solutions for Engineering Problems*, C.C. Berndt, Ed., ASM International, 1996, p 477-482
20. K. Moriya, H. Tomino, Y. Kandaka, T. Hara, and H. Ohmori, Sealing of Plasma-Sprayed Ceramic Coatings by Sol-Gel Process, *Thermal Spray Industrial Applications*, C.C. Berndt and S. Sampath, Ed., ASM International, 1994, p 549-553
21. H. Ito, R. Nakamura, and M. Shiroyama, Infiltration of Copper into Titanium-Molybdenum Spray Coatings, *Surf. Eng.*, Vol 4 (No. 1), 1988, p 35-38
22. A. Ohmori, Z. Zhoue, and K. Inoue, Improvement of Plasma-Sprayed Ceramic Coating Properties by Heat-Treatment with Liquid Mn, *Thermal Spray Industrial Applications*, C.C. Berndt and S. Sampath, Ed., ASM International, 1994, p 543-548
23. A. Ohmori, Z. Zhoue, K. Inoue, K. Murakami, and T. Sasaki, Sealing and Strengthening of Plasma-Sprayed ZrO_2 Coating by Liquid Mn Alloy Penetration Treatment, *Thermal Spraying—Current Status and Future Trends*, A. Ohmori, Ed., High Temperature Society of Japan, 1995, p 549-554
24. "Determination of Viscosity with Höppler Viscosimeter," SFS 3758, Finnish Standards Association, 1977; DIN53015; SIS 02 35 13 (in Finnish)
25. "Methods of Testing Advanced Technical Ceramics—Part 2: Determination of Density and Porosity," prEN 623-2:1991, CEN European Committee for Standardization
26. "Standard Practice for Conducting Dry Sand/Rubber Wheel Abrasion Tests," ASTM G 65-94